Supplemental Materials

Supplemental Figure I.

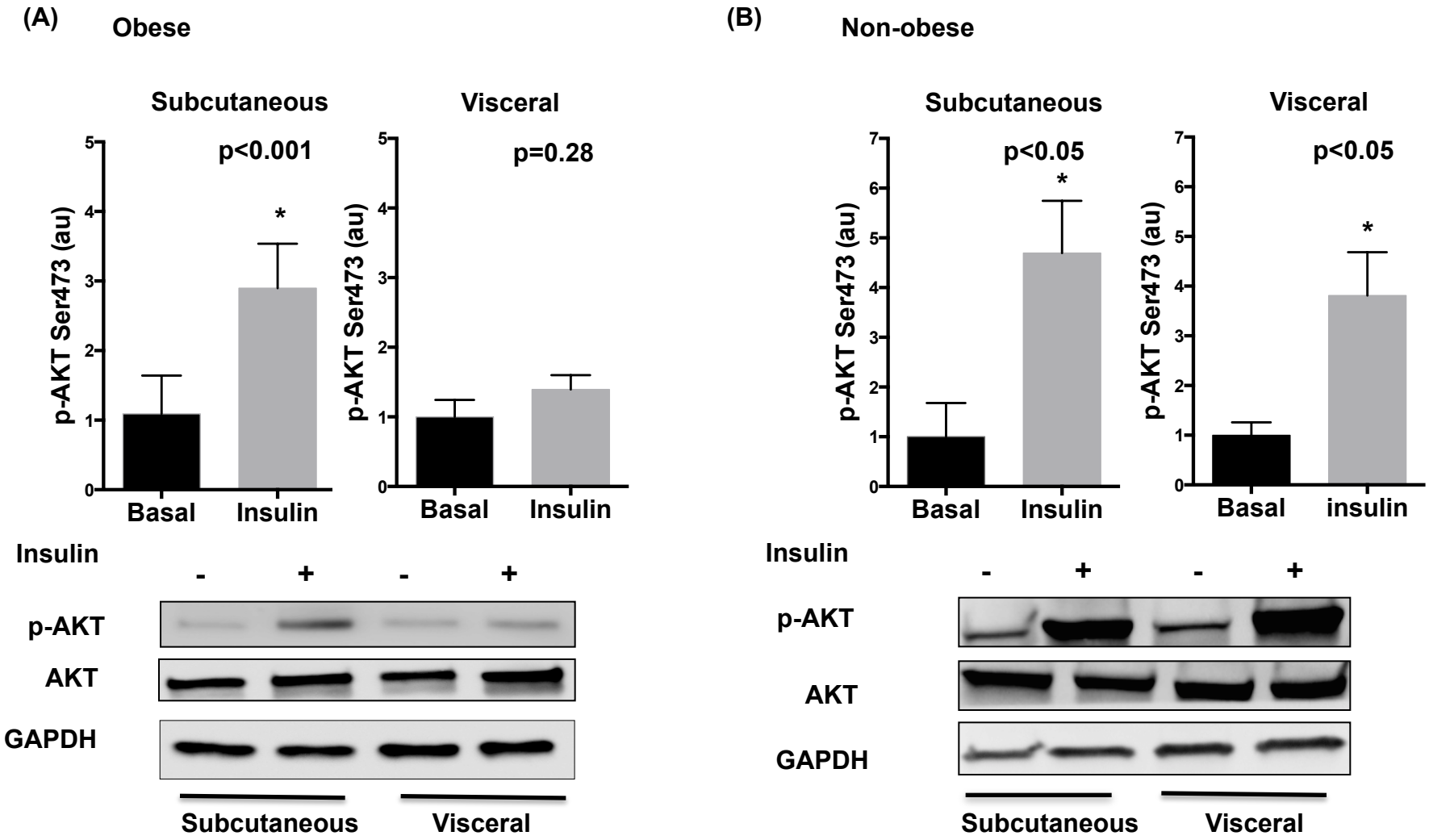

Supplemental figure I: Insulin-mediated activation of AKT in subcutaneous and visceral fat .
A) Visceral adipose tissue from obese individuals exhibited impaired insulin mediated activation of AKT at serine473 (n=10, p=0.28), whereas AKT phosphorylation was intact in subcutaneous fat (n=10, p<0.001). **B)** Insulin mediated p-AKT at serine473 was preserved in both the visceral and subcutaneous fat tissue of non-obese subjects (n=7, p<0.05). Data are presented as arbitrary units (au), indexed to 1 as the basal condition. Data presented as mean ± SEM. GAPDH = control band.

Supplemental Figure II.

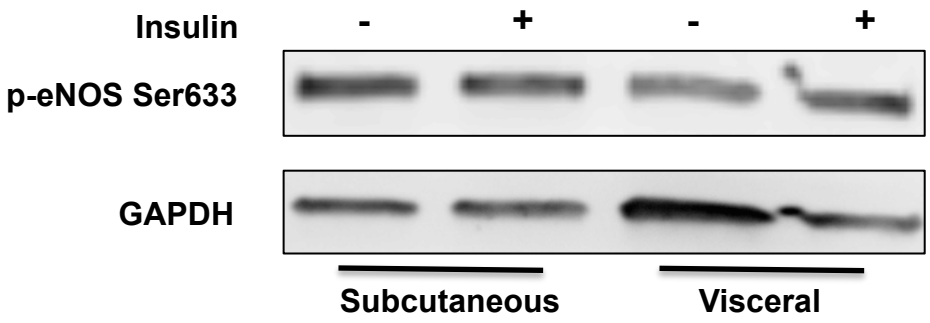

Supplemental figure II: Effect of insulin on Serine633 phosphorylation.
Representative immunoblot demonstrating that insulin had no significant effect on phosphorylation of eNOS at Serine633 in either the subcutaneous or visceral depot of obese subjects (n=4). GAPDH = control band.

Supplemental Figure III.

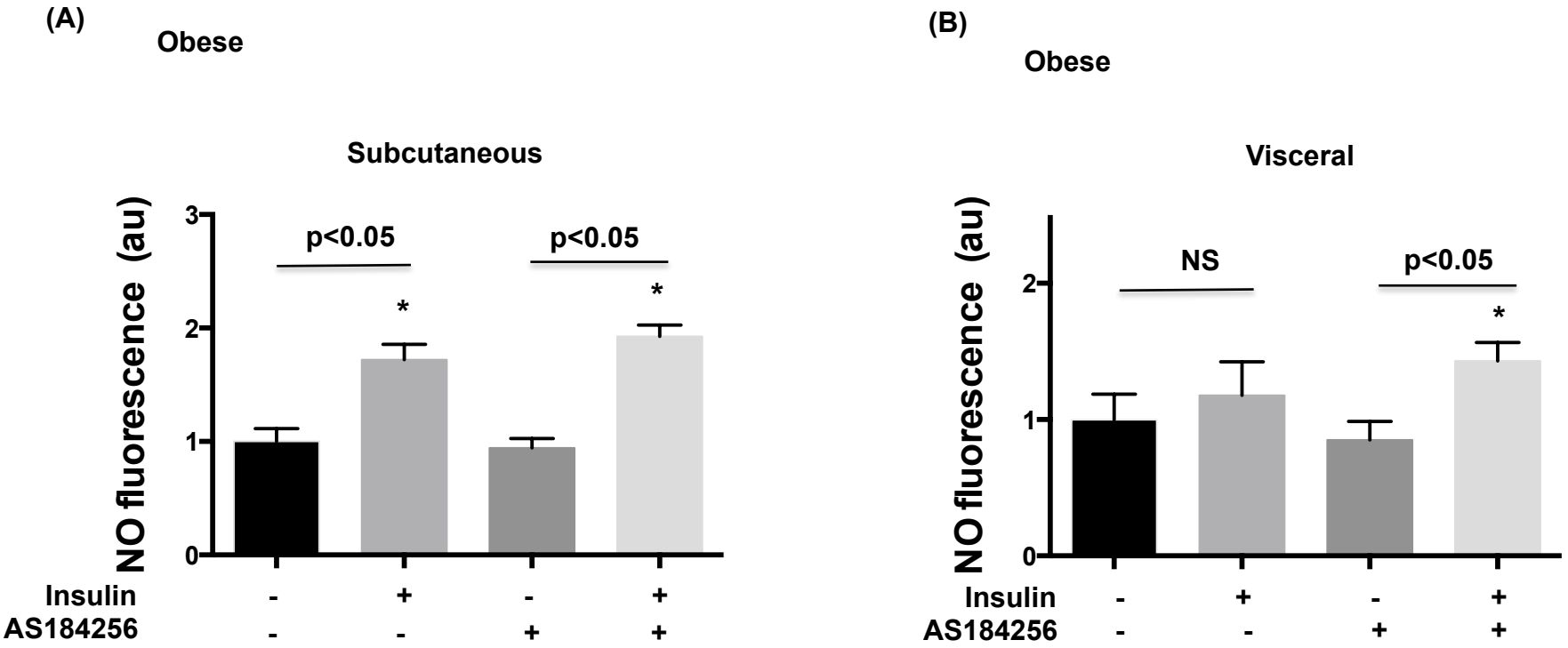

Supplemental figure III: Effect of FOXO-1 antagonism and insulin on nitric oxide (NO) production in endothelial cells from the subcutaneous and visceral fat of obese individuals.
A) NO production by endothelial cells isolated from the subcutaneous depot significantly increased with insulin stimulation. FOXO-1 antagonism by pharmacological inhibition (AS1842856) did not have any significant added effect (n=6, $p<0.05$). **B)** Endothelial cells from the visceral depot exhibited blunted NO production with insulin stimulation. This impairment was restored with FOXO-1 antagonism (n=6, $p<0.05$). Data are presented as arbitrary NO fluorescence units (au), indexed to 1 as the basal condition. Data are presented as mean ± SEM.

Supplemental Figure IV.

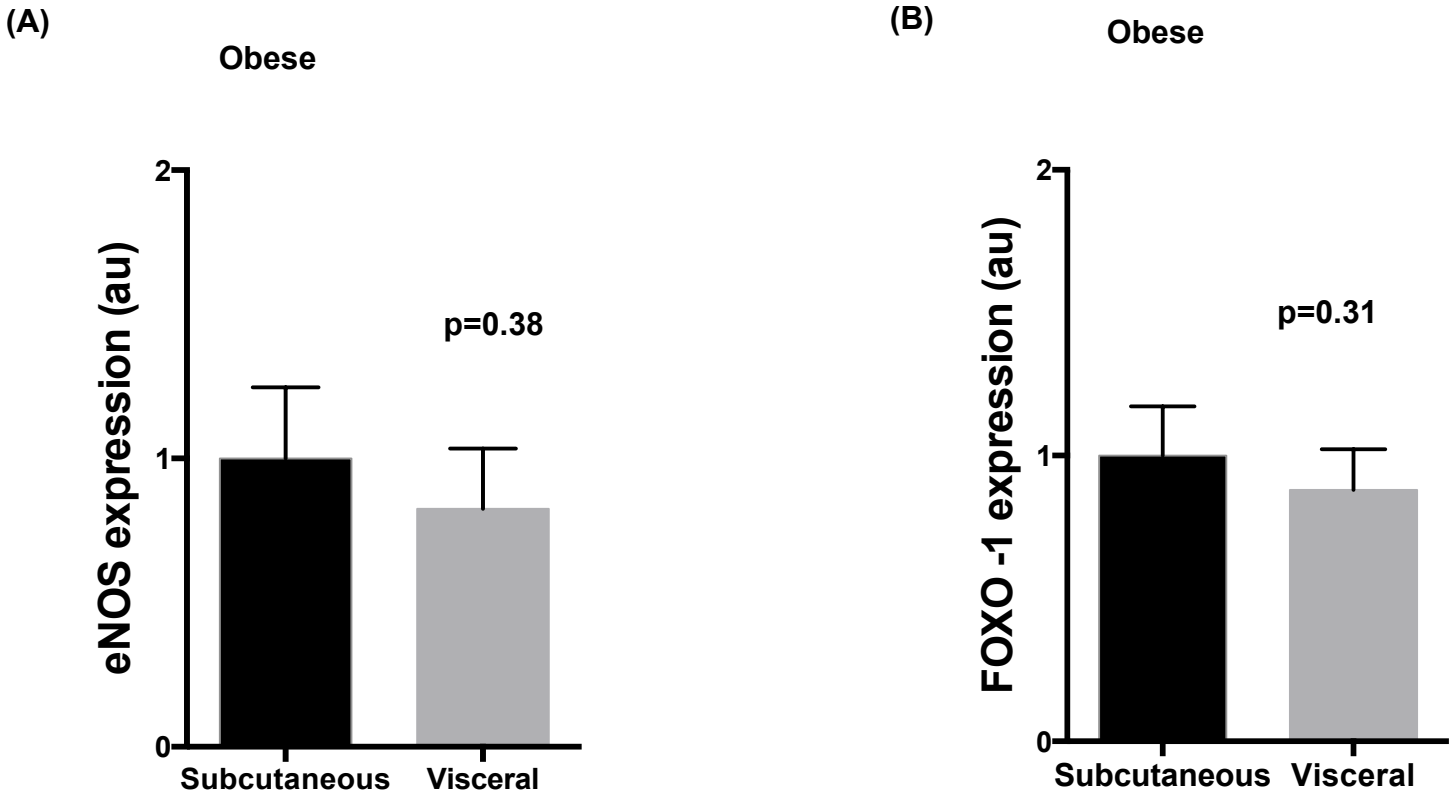

Supplemental figure IV: Total protein quantification in isolated endothelial cells comparing subcutaneous to visceral depots in obese subjects
A) Total eNOS protein expression was the same in subcutaneous and visceral adipose endothelial cells of obese individuals (n=8, p=0.38).
B) Total FOXO-1 endothelial protein expression between depots was also not different (n=13, p=0.31). Data represent quantitative immunofluorescence, presented as arbitrary units (au), indexed to 1 as the subcutaneous depot. Data presented as mean ± SEM.

Supplemental Figure V.

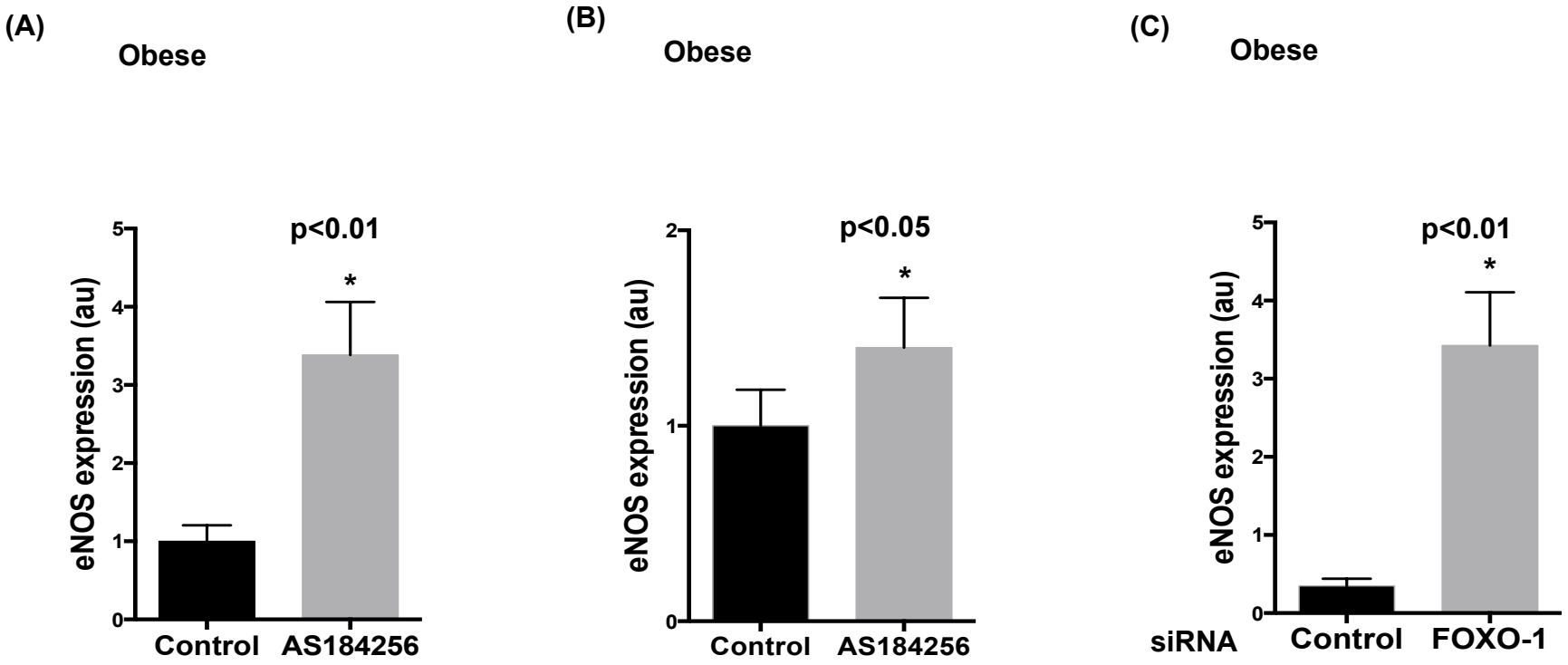

Supplemental figure V: Effect of FOXO-1 antagonism on basal eNOS expression in the visceral fat of obese individuals. **A)** Total eNOS protein expression using western blot in the visceral fat of obese individuals was significantly increased after pharmacological (AS1842856) inhibition of FOXO-1(n=7, $p<0.01$). **B)** Total eNOS protein expression using immunohistochemistry was significantly increased in isolated endothelial cells from the visceral depot of obese subjects after pharmacological inhibition of FOXO-1(n=7, $p<0.05$). **C)** Total eNOS protein expression using western blot was significantly increased in visceral adipose tissue after siRNA mediated knockdown of FOXO-1 (n=9, $p<0.01$). Data are presented as arbitrary units (au), indexed to 1 as the control condition. Data presented as mean ± SEM.

Supplemental Figure VI.

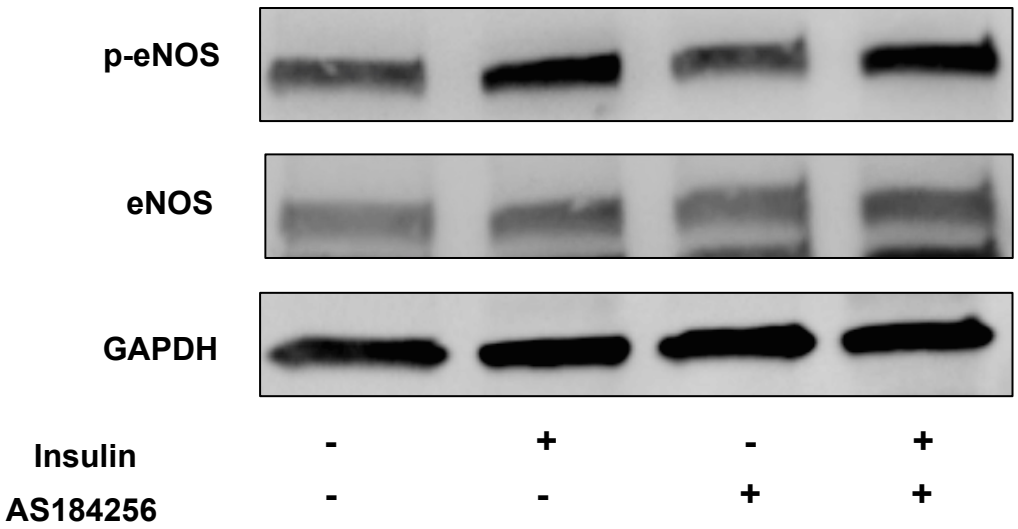

Supplemental figure VI: FOXO-1 antagonism did not significantly alter Serine1177 phosphorylation of eNOS in the subcutaneous depot of obese subjects.
Representative Western immunoblot demonstrating lack of an effect of AS184256 in the subcutaneous depot (n=5). GAPDH= control band.

Supplemental Figure VII.

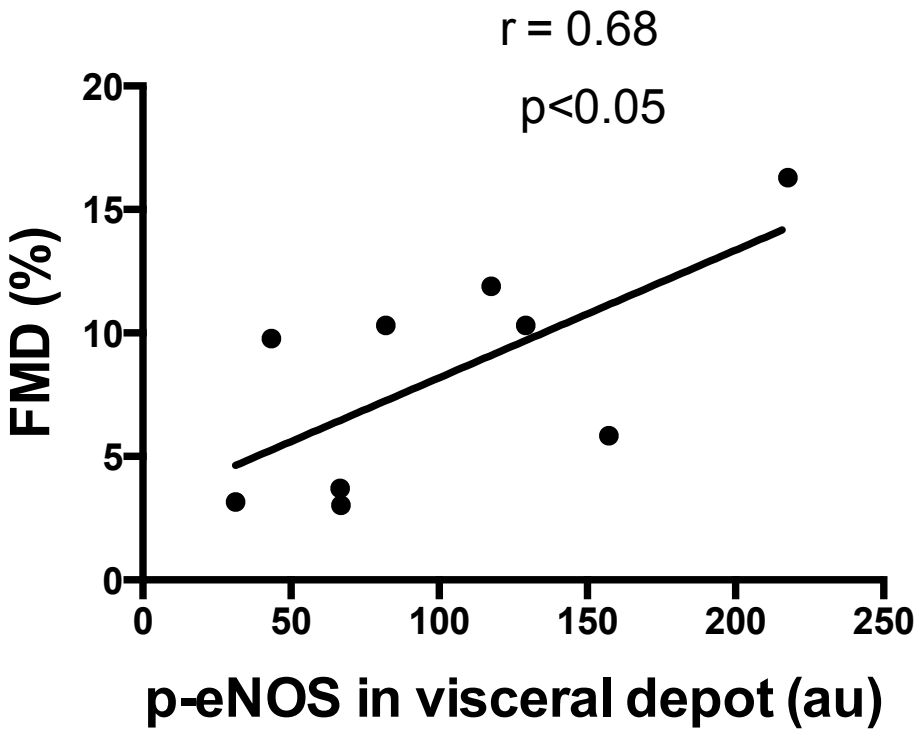

Supplemental figure VII: Basal p-eNOS protein expression in visceral adipose endothelial cells correlated significantly with systemic brachial artery endothelium-dependent flow-mediated dilation (FMD) in obese subjects (n=9).